PROCEEDINGS, 41st Workshop on Geothermal Reservoir Engineering
Stanford University, Stanford, California, February 22-24, 2016
SGP-TR-209

Evaluation of Factors Controlling the Concentration of Non Condensable Gases and their Possible Impact on the Performance of Wells in the Olkaria

Ruth Nelima Wamalwa

Wamalwarn2000@gmail.com, rwamalwa@kengen.co.ke

Keywords: chiller, solveq, gas species

ABSTRACT

The Olkaria geothermal field is located in the Kenyan Rift valley, about 120 km from Nairobi. It is surrounded by other geothermal prospects, such as Suswa, Longonot and Eburru. Development of geothermal resources in the Olkaria area, a high temperature field, started in the early 1950s. Subsequent years saw numerous expansions with additional power plants being installed in Olkaria. These include a binary plant at Olkaria South West (Olkaria III) in 2000, with a capacity of 110 Megawatts (MW), a condensing plant at Olkaria North East (Olkaria II) in 2003, with a capacity of 105 MWe and another binary plant at Olkaria North West (Oserian) in 2004, with a capacity of 2 MWe. Another 280 Mw was commissioned in the year 2014 within East production field (EPF) and Olkaria Domes (OD) areas.

The study considered samples from 4 producing wells from 3 fields the Olkaria geothermal area (OW-44 from the Olkaria East, OW-724A from the Olkaria North East and OW-914 and OW-915 from the Olkaria Domes field). The chemical data was first analyzed using SOLVEQ. This helped in the determination of the equilibrium state of the system, the reservoir temperatures and the total moles to be run through Chiller. The chiller runs considered the processes that have been proven to be occurring in the Olkaria field i.e., boiling and condensing processes, fluid-fluid mixing rocks and titration resulting from water-rock interaction. The effects on gas evolution were evaluated by looking at the resulting recalculated gas pressures.

The results indicate that the gas species are not in equilibrium with the mineral assemblages due to processes of boiling, condensation and mixing. The chiller evaluation show boiling as the major process leading to evolution of gases. OW-44 had the least gas concentrations arising from the considered reservoir processes due to degassing and near surface boiling besides the removal of NH_3, H_2 and H_2S through reaction with steam condensate. The gas breakout is most likely in OW-914 and least in OW-44. The study proposes different reservoir management strategies for the different parts of the Olkaria geothermal field. That is by increasing hot reinjection in the eastern sector around well OW-44. The reservoir around OW-914 to be managed by operating the wells at a minimum flow rate (or even to close them) or use of chemical inhibitors to prevent calcite scaling.

1. INTRODUCTION

Evaluation of gases concentration in Olkaria geothermal field (West JEC, 2009) revealed that on average the gases are highest in the Domes, intermediate in Northeast production field and lowest in East production field well fluids. This is considered to be the primary cause of zonation of HCO_3/Cl among the well fluids from the three fields. West JEC (2009) considered three options i) CO_2 gets added at great depth to Northeast production field and Domes waters as a result of volcanic degassing below these areas, with less input of deep CO_2 to the East production field; ii) deepest CO_2 is similar in all three areas, but waters of the East production field lost CO_2 during the onset of deep boiling such that the CO_2 escapes to fumaroles which lie west and south of the East production field iii) cap-rock conditions in the Northeast production field and Domes are somewhat more restrictive than in the East production field, leading to more entrapment at shallower levels of CO_2 that has been released by deep boiling.

Gases in particular CO_2, H_2S, H_2 and CH_4 are common major solutes in fluids of volcanic geothermal systems like Olkaria (Kenya), Mahanagdong (Philippines) and Nesjavellir, Hellisheidi and Krafla (Iceland) (Arnorsson et al., 2010 and Angcoy, 2010). Their concentration in systems that are unexploited is generally controlled by temperature dependent equilibria with various mineral buffers (Giroud and Arnorsson, 2005). This results in variation in gas concentration with temperature. Giroud and Arnorsson, (2005) added that for geothermal systems with average reservoir temperatures of between 230-300°C, a case of Olkaria, their CO_2 buffer is considered to be clinozoisite + prehnite + quartz + calcite whereas that of H_2S buffer to be pyrite + pyrrhotite + epidote + prehnite. In highly saline waters, the H_2S mineral buffer consists of pyrite + magnetite + hematite. The gas ratios like in the case of H_2S/H_2 activity ratio correspond closely to equilibrium with the mineral pairs of pyrite/pyrrhotite and pyrite/magnetite that is generally under saturated with respect to the individual minerals. These findings agree with Karingithi (2002) in the study on the Olkaria field which found out that activity of aqueous H_2 and H_2S gases generally corresponded closely to equilibrium with the mineral buffer pyrite/pyrrhotite/magnetite. The activities of these two also corresponded closely to equilibrium with the mineral buffer pyrrhotite-prehnite-epidote-pyrite. The H_2S/H_2 activity ratio corresponded closely to equilibrium with the mineral pair pyrite/pyrrhotite and pyrite/magnetite. However, the challenge lied in the conclusively identifying which buffers controlled the activities of aqueous H_2.

The concentrations of gases in a geothermal field under exploitation are higher than those of the parent fluid. The value is frequently in the range 50-300 and 2-20 mmoles/kg of steam for CO_2 and H_2S respectively (Giroud and Arnorsson, 2005). This variation is dependent

on their concentration in the parent geothermal water, the steam fraction, the steam separation pressure and the boiling processes. According to Giroud and Arnorsson, (2005), long-term utilization of geothermal reservoirs may lead to decline in the concentrations of CO_2 and H_2S in the steam. This decline may be caused by recharge of cooler water into producing aquifers and/or progressive boiling of water retained in the aquifer by capillary forces. Enhanced boiling, which is a consequence of reservoir pressure draw down and steam separation during lateral flow into production wells may cause the well discharge to become depleted in gas. In case of a two phase reservoir, the gas concentrations tend to be higher compared to concentrations at a particular temperature mostly due to processes of boiling and formation of steam caps in the reservoir and/or enhance fumarolic activity. Karingithi (2002) also notes that gas samples from marginal wells whose discharge fluid are mixed with non-geothermal fluid show low H_2 and H_2S values with respect to the equilibrium with the mentioned buffer.

The gases form major factors that affect the reservoir pressure in the deep liquid-dominated geothermal reservoirs (Haizlip et al., 2012). Haizlip et al., (2012) further added that under static conditions, pressure in most producing aquifers around the world ranges between 130 to 230 bars at depths between 1700 to 2800m. The temperatures in this region range between 219 to 242°C. The effect of the gas pressures on a well performance is evaluated in terms of the gas breakout pressure i.e. the pressure below which the fluids begin to transform into two-phase. According to (Haizlip et al., 2012) gas breakout pressure is the sum of the gas pressure and water pressure at the reservoir temperature. In most cases, due to pressure drop, thermal fluids start to boil leading to degassing of CO_2 while fluids rise in a wellbore. In bicarbonate type of waters, this leads to the fluid becoming saturated with calcite as a result of both CO_2 exsolution and calcium and carbonates.

For a field that is under utilization like Olkaria, changes in the gas content of well discharges with time help in providing valuable information about the response of the reservoir to the production load (Karingithi, 2002). This is in respect with processes such as cold recharge resulting to fluid-fluid mixing, volcanic degassing and enhanced boiling (Gudmundsson and Arnorsson, 2002; Kissling et al., 1996 and Armannsson, 2003). In this study an evaluation of reaction processes controlling the concentration of prevalent reactive gases CO_2, H_2S, H_2, CH_4 and N_2 in Olkaria well discharges are determined. The procedure involve first the determination of the equilibrium state between fluids and rocks using the software package SOLVEQ followed by determination of reaction processes in aqueous-mineral-gas systems using the software package CHILLER (Reed et al., 2012a and b). The software package SOLVEQ/CHILLER, have been preferred due to its applicability for studying multiphase systems as well undergo boiling and mixing processes (Bienkowski *et.al.* 2003). This issue is relevant for the long-term release of gases from geothermal power plants. Ideas are given with respect to geochemical monitoring of geothermal reservoirs under utilization with the purpose of predicting possible decline in gas emissions. Then the results are evaluated against the measured pressures through the downhole temperature and pressure surveys to determine if there are chances of gas breakout occurrence.

2. GENERAL SETTING OF THE STUDY AREA

The Olkaria Geothermal area is located within the Olkaria central volcanic complex in the central sector of the Kenyan Rift Valley. The complex is located south of Lake Naivasha, approximately 120 km from the capital city Nairobi. It is bordered by other geothermal prospects, like Suswa, Longonot and Eburru (Figure 1).

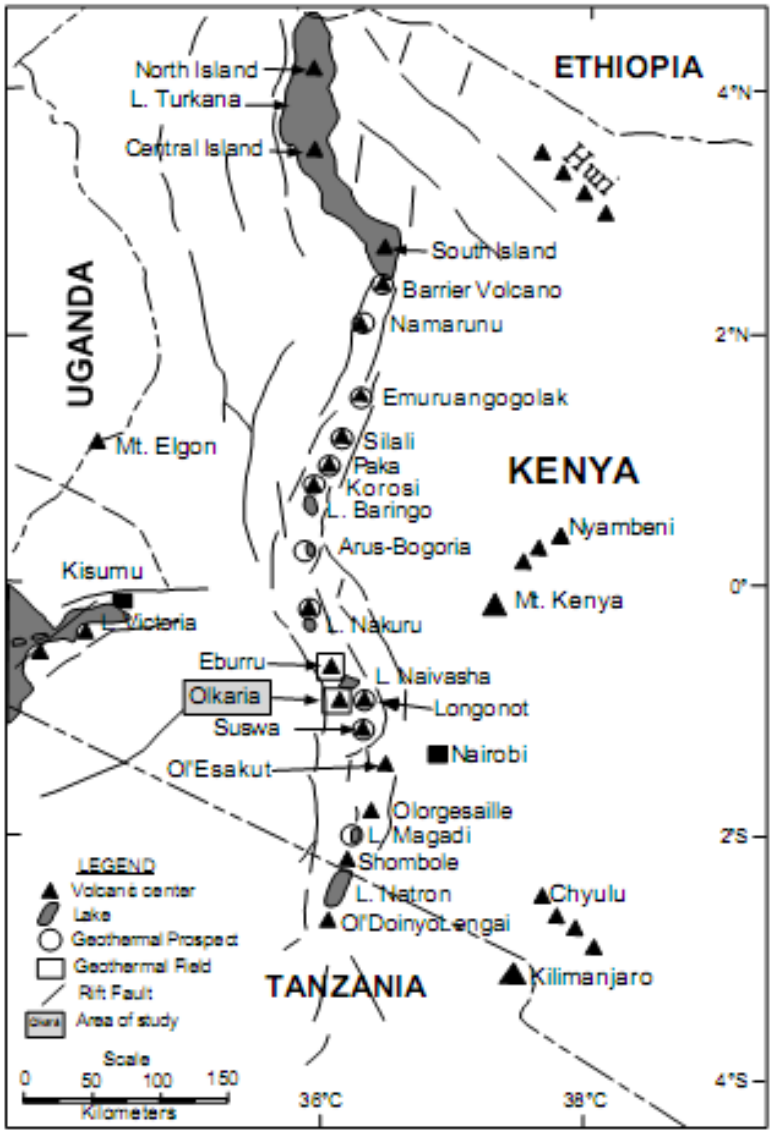

Figure 1: Map of the Kenya rift showing the location of Olkaria geothermal field and other Quaternary volcanoes along the rift valley (Lagat, 2004).

This geothermal area covers approximately 140 km^2 and it is divided into seven fields, namely: Olkaria East, Olkaria Northeast, Olkaria Central, Olkaria Northwest, Olkaria Southwest, Olkaria Southeast, and Olkaria Domes for ease of exploitation (Figure 2). The fields are in different stages of exploitation. The completely explored fields are Olkaria East, Olkaria Northeast and Olkaria Southwest while Olkaria- Domes is the recent of them all where exploitation for power production started in the year 2014 whereas Olkaria Southwest is yet to be developed.

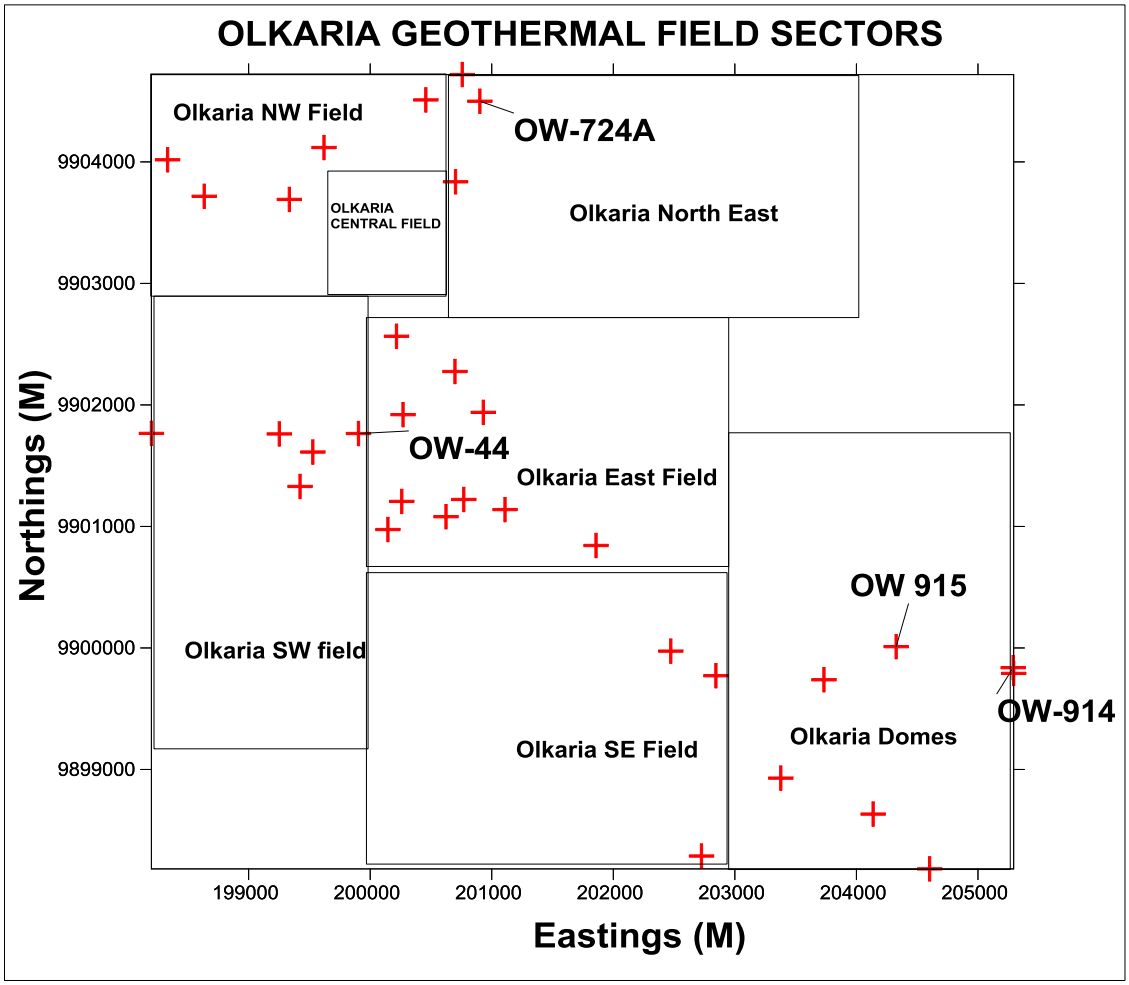

Figure 2: Geothermal fields within the Greater Olkaria geothermal area (KenGen, 1999). The red crosses indicate the location of wells. Labeled wells are the ones used in this study.

The Olkaria East Field is located on the East of the Olkaria hill (Figure 3) and has been under steam exploitation since 198 through the Olkaria 1 power plant. This power plant is served by 31 wells connected to the steam gathering system out of 33 wells drilled. As of end of 2014, the steam was being harnessed from 22 as 9 wells had become non-commercial producers due to decline in output over time. Two of these wells, OW-6 and OW-3 are being used as reinjection wells whereas OW-11 was recently commissioned to take low pressure (LP) brine from OW-2, 27, 31 and 33 in March, 2015. The field also hosts newly drilled wells for the Olkaria1 unit IV and V power plant like OW-35, OW-36A OW-37A, OW-38, OW-38A, OW-41, OW-42A and OW-44, OW-44A and OW-44B. The power plant was commissioned in October, 2014. This is besides well OW-37A, OW-43 and OW-43A which are connected to a wellhead generator.

The Olkaria North East field has been used for power generation since October 2003. It has a total of 20 wells that are connected to the steam gathering system. Of the twenty, 6 wells (OW-709, OW-710, OW-712, OW-713, OW-718 and OW-721) have individual separators while the other 14 wells (OW-701, OW-727, OW-705, OW-725, OW-706, OW- 711, OW-707, OW-715, OW-714, OW-716, OW-719, OW-726, OW-720 and OW-728) share separators. Four wells are used for hot re-injection i.e. OW-R2, OW-R3, OW-703 and OW-708. Wells OW-704, OW-717, OW-723 and OW-724 are non-producers and are currently used for pressure monitoring (Figure 1).

Olkaria-Domes Field lies to the west of Longonot Volcano and on the SE of the Olkaria hill (Figure 3). It was the last of the 7 sectors to be explored by deep drilling. Here, three deep exploration wells were drilled between 1998 and 1999. Drilling was halted for close to eight years due to shortage of funding but resumed in June 2007. This led to realization of 140 Mwe power plant commissioned in October, 2014 using wells OW-910, OW-910A, OW-910B, OW-908, OW-908A, OW-908B and OW-909, OW-915, OW-915A, OW-915B, OW-916 and OW-912. This is besides the wellheads at OW-914 pad which generate a total of 27.8 Mwe.

2.1 Geological features and physical characteristics of the reservoir

2.1.1 Geology of Olkaria volcanic complex

Olkaria volcanic complex does not have a clear caldera association (Naylor, 1972, Virkir, 1980, Clarke et al., 1990 and Mungania, 1992). Lagat et al., (2005) however concluded that the presence of a ring of domes in the east and south, and southwest can be used to infer to the presence of a buried caldera. Other adjacent volcanic centers like Longonot volcano, Suswa caldera and the Eburru are associated with calderas of varying sizes.

The downhole geology in geothermal wells in Olkaria field has helped to reveal the lithostratigraphy of the area (Omenda, 2000). From this study, the regional geology has been divided into six main lithostratigraphy groups which are Proterozoic "basement" formations, Pre-Mau volcanics, Mau tuffs, plateau trachytes, Olkaria basalt and Upper Olkaria volcanics (Omenda, 2000). The basement rocks comprise of Proterozoic amphibolite facies grade gneisses, schists, marble and quartzites of the Mozambique group (Shackleton, 1986, Smith and Mosley, 1993). The Mau tuffs are the oldest seen on the surface in the Olkaria area. They are common in the outcrops and wells west of Olkaria Hill, but not evident for their occurrence in the east is available. Omenda (1994 and 2000) concluded that this might be due to an east dipping high angle normal fault that is cutting through the Olkaria Hill. The Upper Olkaria volcanic are overlain by Olkaria basalt in the area to the east of Olkaria Hill while the formation is absent to the west. This formation consists of basalt flows and minor pyroclastics and trachytes and varies in thickness from 100 m to 500 m (Omenda, 2000).

The Upper Olkaria formations comprise of mainly lavas and ashes from Suswa and Longonot volcanoes (Thompson et al., 1963, Ogoso-Odongo, 1986, Clarke et al., 1990, Omenda, 2000). Their occurrence is between 0 and 500m depths below surface. The youngest of these lavas is the Ololbutot comendite, which, has been dated to about 180 years (Clarke *et al.*, 1990).

2.1.2 Structural setting of the Olkaria volcanic complex

Structures in the Olkaria geothermal area include the ring structure, the Ol'Njorowa gorge, the Gorge Farm fault, the ENE-WSW Olkaria fault and NW-SE trending faults (Figure 3). These faults are prominent in the East, Northeast and West Olkaria fields unlike in the Olkaria Domes area, most probably due to the thick pyroclastics cover in this area (Clarke et al., 1990). The NW-SE trending faults are thought to be the oldest and are associated with the development of the rift and are associated with hot chloride rich fluids except for the Gorge Farm fault, which bounds the geothermal fields in the northeastern part and extends to the Olkaria Domes area. The most recent structures are the NNE-SSW faults. They are thought to be young and carry cold, low chloride content fluids.

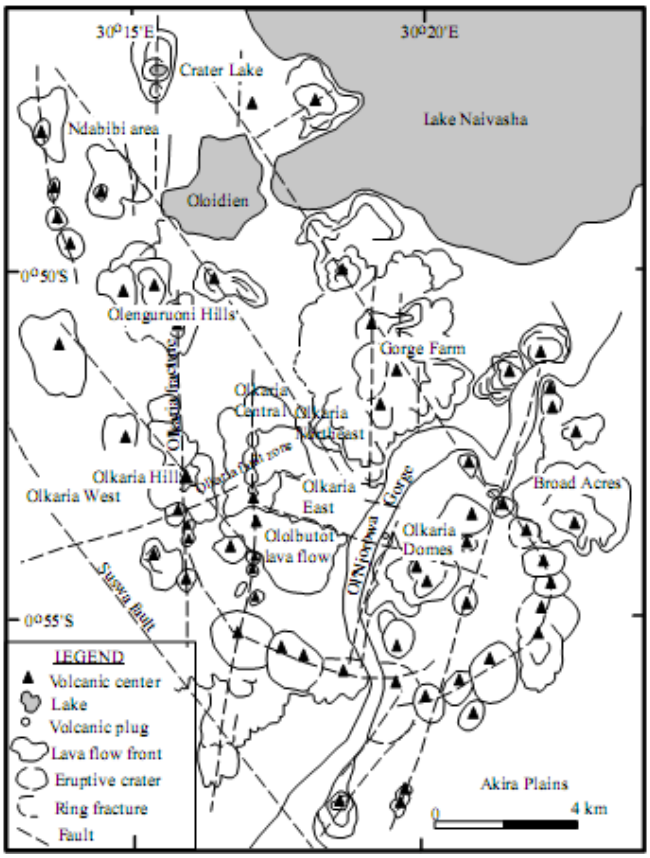

Figure 3: Volcano-tectonic map of the Greater Olkaria volcanic complex (modified from Clarke *et al.*, 1990)

The craters located on the northern edge of the Olkaria Domes area characterize the magmatic explosions, which occurred in submerged country (Mungania, 1992). These craters are arranged along a row where the extrapolated caldera rim trace passes. Dike swarms exposed in the Ol'Njorowa gorge trend in a NNE direction further confirming the reactivation of recent faults with this trend. The development of the Ol'Njorowa gorge is thought to have been initiated by faulting along the trend of the gorge but the feature as it is today resulted from catastrophic outflow of Lake Naivasha during its high stands (Clarke et al., 1990). The volcanic plugs (necks) and felsic dikes occurring along the gorge further contributes to the evidence that the fault controls the development of this feature. Subsurface faults have been encountered in most Olkaria wells (KenGen, 2000).This is witnessed mostly in wells that encountered drilling problems when these faults were dissected due to collapse and loss of drilling fluids and cement. Materials recovered from these zones were mainly fault breccias.

3. RESERVOIR CHARACTERISTICS

3.1 Reservoir pressure and temperature characteristics

Studies on the temperature and pressure distribution in the entire field indicate that fluid movement in the Olkaria geothermal system is tectonically controlled (Ofwona, 2002). The reservoir temperatures reach as high as 380°C at 3400 meters depth in well OW-49 in Olkaria East. The Olkaria East and North East have a two-phase reservoir (reservoir has steam water mixture feed zone) at least to the depth penetrated by the deepest wells whereas the Olkaria Domes has a liquid dominated reservoir without a steam cap (Ambusso and Ouma, 1991; KenGen 1999). The pressure decreases both eastwards and westwards from respective peaks towards Olkaria Central (Figure 4). Within the Olkaria Central and Northeast, the pressures decline southwards towards well OW-401 and towards Olkaria East, respectively (Ouma, 1999).

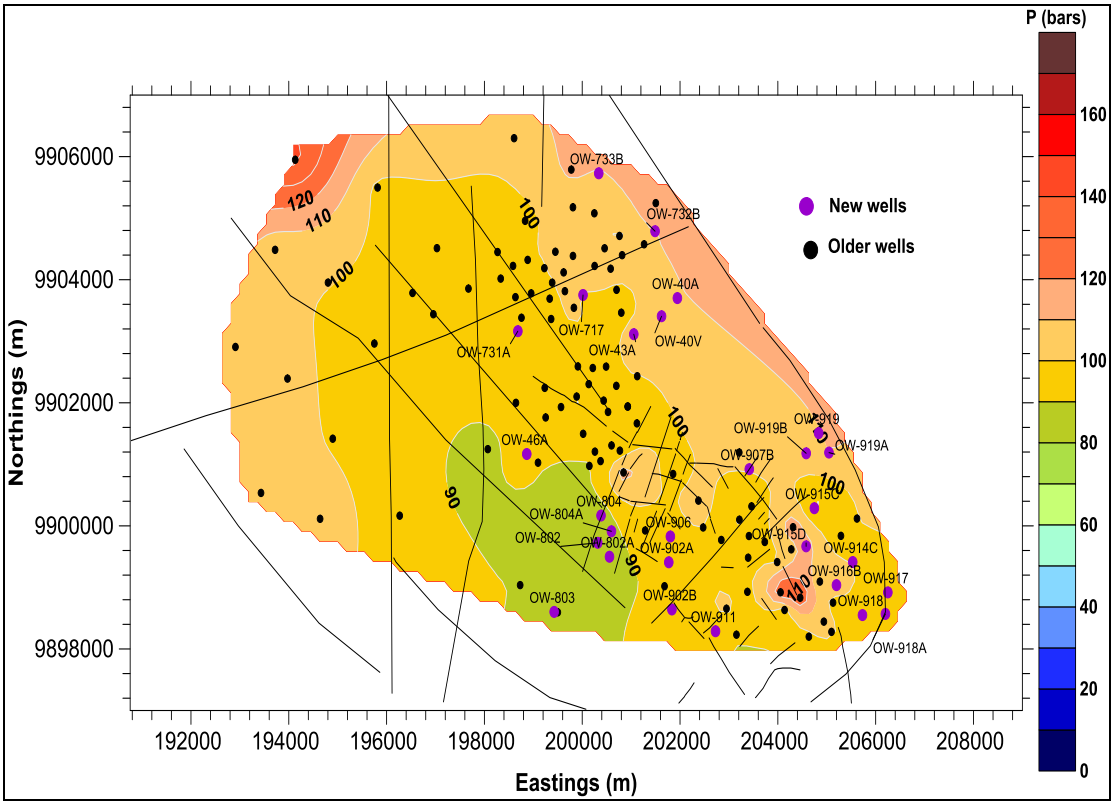

Figure 4: Measured Pressure variations for the Olkaria geothermal field.

On the individual wells of interest, as shown in profiles in Figure 5, OW-44 was drilled to 3000m in early 2011. It has a high injectivity index 164 lpm/bar and bottom hole temperatures of about 300°C. Its major feed zones are observed around 760m and 2250m while minor ones at 1500m and 1750m depths. OW-724A just like OW-44 was drilled to a depth of 3000m but in early 2012. It has slightly higher injectivity than OW-44 at about 180 lpm/bar. Major feed zones in this well is at 1800m and minor ones are observed around 1400m, 1750m, 2000m, and 2550m depths as indicated by the heat up temperature profiles. The pressure profiles indicate that the water rest level was at 550m during pre-injection. There is a pivot point at around 1800m depth hence the major feed zone is around 1800m depth. The pressure profiles indicate that the water rest level was at 550m during pre-injection.

OW-915's (in the Olkaria Domes field) temperature profile plot indicates minor feed zone between 1200m and 1500m and a major feed zone at 2300m meters depth. The pre-injection data shows a water rest level at approximately 300m depth. The rapid shift of the pressure curves from the right to the left as heating (recovery) continued at the well bottom and near the top is a manifestation of the accumulation of the steam in the well bore hence low pressure. The well has low injectivity compared to OW-44 and OW-724A at 145lpm/bar.

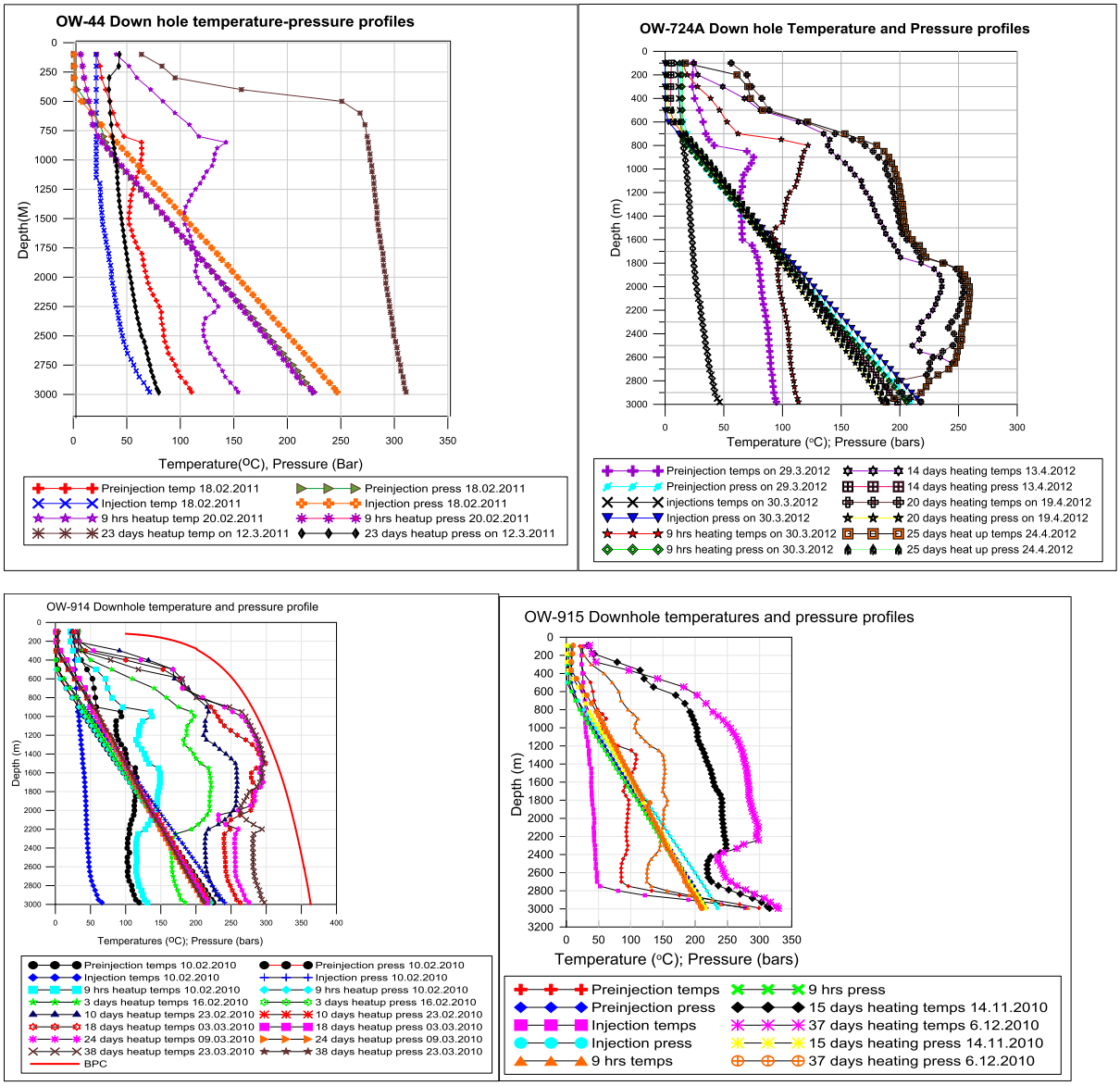

Figure 5: OW-44, OW-724, OW-914 and OW-915 down hole temperature and pressure profiles.

3.2 Reservoir fluid chemistry

The Olkaria wells discharge fluids with enthalpy ranging from1000kJ/kg to 2750kJ/kg (Karingithi 2002). Wells in the East production field have excess discharge enthalpy. This implies that the enthalpy of discharged fluid is higher than that of steam-saturated water at the respective aquifer temperatures. The water discharged from wells in the Olkaria field is low in dissolved solids compared to water from most other drilled high-temperature geothermal fields in the world with Chloride concentrations in water at the weir box ranges between 50 and 1100 ppm (Karingithi, 2000). The water from wells in Olkaria East and Northeast (refer to Figure 2) tend to be highest in chloride. According to Karingithi (2002) the high chloride could be as a result of up flow of deep high-temperature geothermal fluid, although progressive boiling by heat flow from the rock may also be a contributing factor.

A study by Wambugu, (1995) established that in Olkaria West field the chloride concentrations are quite low except in well OW-305, which discharges water similar to that discharged from the wells in the Olkaria East and Olkaria Northeast fields. Well OW-305 is therefore thought to be tapping of the up-flow fluid for Olkaria West field. The relative abundance of chloride, sulfate and bicarbonate plots show that wells in the Olkaria East production field and in Olkaria Northeast discharge sodium-chloride type water while the Olkaria Domes fields discharge a mixture of chloride and bicarbonate end- member water (Figure 6).

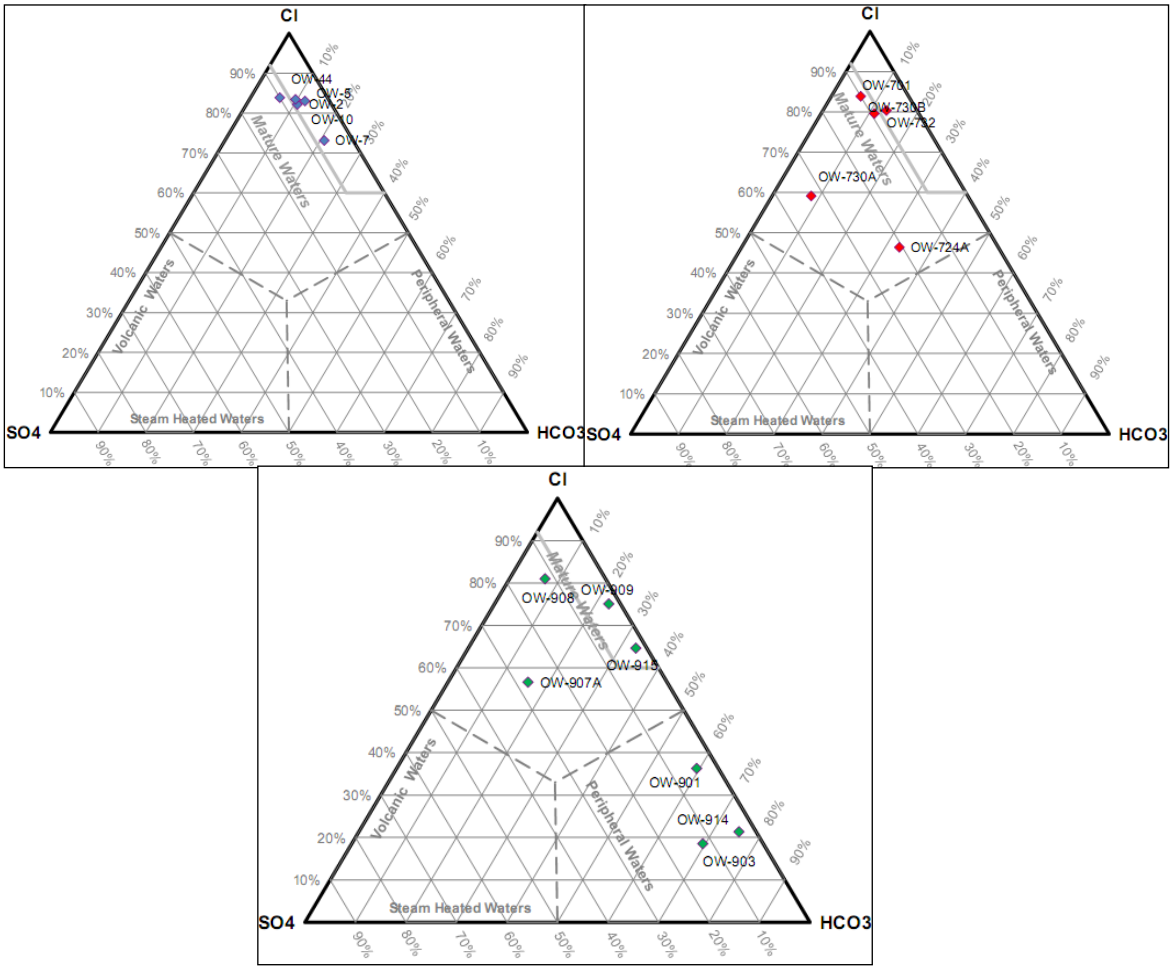

Figure 6: Cl-SO_4-HCO_3 ternary for the Olkaria geothermal field. The blue symbols are for the East field, red ones for the NE field while the green ones are for the Olkaria Domes.

The water from the weir box of the Olkaria wells is slightly to moderately alkaline (pH 8.1-9.9 as measured at 20^{o}C) and is relatively high in bicarbonate (Wambugu, 1995). The bicarbonate concentration is in the range of with 90-13000 ppm with distinctly highest carbon dioxide found in the Olkaria West field followed by the Olkaria Domes. Wambugu (1995) added that this could be a consequence of CO_2 supply to the geothermal fluid and a subsequent reaction between the carbonic acid and minerals of the rock leading to evolution of CO_2 gas.

Geochemical conceptual Model

The geochemical data identifies upflow zones in the areas around OW-701, OW-711 and OW-705 in the Olkaria North East field, OW-38, OW-32, OW-35A and OW-39A for the Olkaria East field and in the Olkaria Domes area in wells OW-908, OW-908A and OW-911A (Figure 7). These areas are characterized by chloride water types. Areas around OW-914 and OW-902 have peripheral waters and thus thought to be on the margins of the reservoir. The influence of structures is also apparent with the NW-SE trending faults being associated with high temperature and Cl rich waters. The NE-SW trending faults tend to carry cool temperature waters that have led to decline in enthalpies of the wells it cuts through (Wamalwa et al., 2014). Wamalwa et al., (2014) also added that the faults within the Ol Njorowa gorge (between the Olkaria East and Olkaria Domes) act to carry cool, less mineralized water that tend to dilute the wells in the shallow depths as in the case of OW-21 , OW-22 and OW-23. A deeper well like OW-901 which is 2200 m deeper compared to 1600 m of OW-23 well proves otherwise.

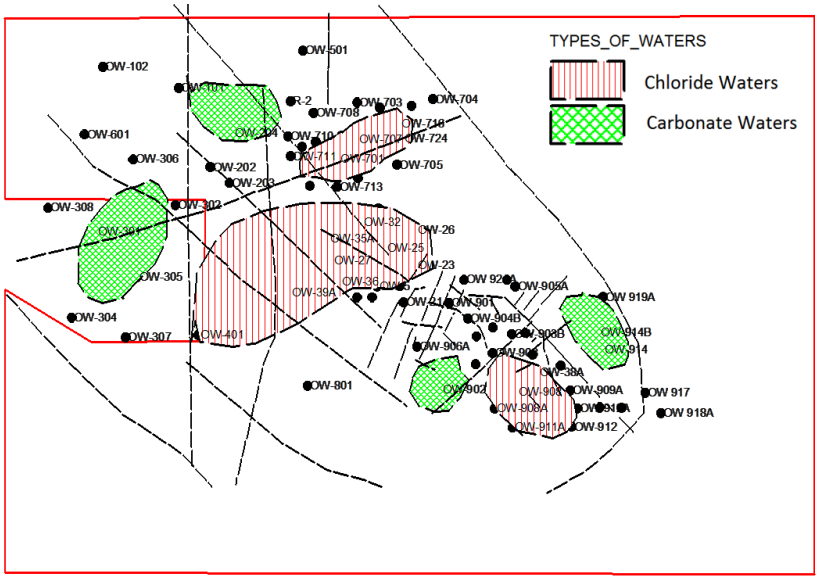

Figure 7: Distribution of the various water types in the Olkaria geothermal area.

4. RESERVOIR CHARACTERISTICS

4.1 Sampling and analysis

The study comprises samples from 4 producing wells of 3 fields out of 7 in the Olkaria geothermal area. The sampling and analysis was carried out by KenGen staff using methods as described by (Arnórsson et al., 2006 and Stefansson et al., 2007). The liquid and vapor phase were separated using a Webre separator connected to the pipe line. Here, care was made to ensure that no condensation occurred upon cooling from the pipe line into and out of the separator.

After the set up, vapor samples were collected into pre-evacuated gas bulbs (100 ml) containing 40% NaOH. CO_2 and H_2S was absorbed in the NaOH solution whereas the non-condensable gases i.e. H_2, N_2, O_2, Ar, CH_4 got concentrated within the gas-head space of the gas bulb. The non-condensable gases were then analyzed within the head space of the gas bulbs using Gas Chromatography (GC) while the concentrations of CO_2 and H_2S were analyzed within the alkaline condensate by titration.

The liquid phase samples were cooled down using a stainless steel spiral that was connected to the webre separator in-line and immersed in a bucket of water. Samples for major cation determination were filtered through 0.2 µm filters into polypropylene bottles and acidified with 0.5% HNO_3 and later analyzed using an Inductively Coupled Plasma (ICP). Samples for major anion and CO_2 determination were filtered through 0.2 µm filters into polypropylene and amber glass bottles and analyzed using ion chromatography (IC). The quality of the sampling and chemical analysis was ensured by using well known standard solutions for calibration, running reference samples before starting the analysis and evaluation of charge balance for the analyses. The samples used had a charge balance between -5 and +5%.

4.2 Data analysis

The chemical data was first run through SOLVEQ to determine the equilibrium state of the system and then through Chiller considering the processes that have been proven to be occurring in the most high temperature geothermal fields (Reed et al., 2012a). These processes include boiling and condensing processes, fluid-fluid mixing and rocks titration resulting from water-rock interaction. Their effect on the evolution of gases is by looking at the resulting recalculated gas pressures.

4.2.1 Equilibrium evaluation

The equilibrium constants were determined using mineral assemblages that potentially controlled the concentrations of H_2S, H_2 and CO_2 in the aquifer fluid using reactions as shown in Table 1 and temperature equations for the equilibrium constants in Table 2. These included thermodynamic data on oxide and silicate minerals as given by Holland and Powell (1998) whereas sulfide minerals were as reported by Robie and Hemingway (1995). The thermodynamic properties of the dissolved gases were based on the solubility constants by Fernandez-Prini et al. (2003) and the standard Gibbs energies of the ideal gases given by Robie and Hemingway (1995). Over the limited pressure range considered, the specific volume of minerals was taken to be independent of temperature and pressure.

TABLE 1: Reaction equations for the equilibrium constants (Arnorsson et al., 2010).

H_2S: 1/3pyr + 1/3pyrr + 2/3pre + 2/3H_2O_l = 2/3 epi + H_2S_{aq}	1
H_2S: 2/3gro + 1/3pyr + 1/3pyrr + 2/3qtz + 4/3H_2O_l = 2/3epi + 2/3wol +H_2S_{aq}	2
H_2S: 2gro + 1/4 pyr + 1/2 mag +2qtz +2H_2O_l = 2epi + 2wol +H_2S_{aq}	3
H_2S: 1/4 pyr + 1/2 pyrr + H_2O_l = 1/4 mag + H_2S_{aq}	4
H2: 4/3 pyrr + 2/3 pre + 2/3 H_2O_l = 2/3 epi + 2/3 pyr + H2,$_{aq}$	5
H_2: 2/3gro + 4/3pyrr + 2/3qtz + 4/3H_2O_l = 2/3epi + 2/3wol + 2/3pyr +$H_{2,aq}$	6
H_2: 6gro + 2mag + 6qtz + 4H_2O_l = 6epi + 6wol + $H_{2,aq}$	7
H_2: 3/2pyrr + H_2O_l = 3/4pyr + 1/4mag + $H_{2,aq}$	8
CO_2: czo + cal + 3/2 qtz + H_2O_l = 3/2 pre + $CO_{2,aq}$	9
CO_2: 2/5 czo + cal + 3/5 qtz = 3/5 gro + 1/5 H_2O_l + $CO_{2,aq}$	10
$CO_{2,aq}$ + 4$H_{2,aq}$ = $CH_{4,aq}$ + H_2O_l	11
H_2S_g = H_2S_{aq}	12
$H_{2,g}$ = $H_{2,aq}$	13
$CO_{2,g}$ = $CO_{2,aq}$	14
$CH_{4,g}$ = $CH_{4,aq}$	15

TABLE 2: Log K-temperature equations for the reactions given in Table 1 above (Arnorsson et al., 2010)

log [H2S] = 13.608 +592324/T^2-9346.7/T -0.043552T +0.000029164T^2+5.139logT	1
log [H2S] = 13.659 +555082/T^2 -9256.6/T -0.043608T +0.000028613T^2 +5.148logT	2
log [H2S] = -0.836 -216659/T^2 -2847.3/T +0.008524T -0.000002366T^2+0.152logT	3
log [H2S] = 13.589 +590215/T^2 -9024.5/T -0.044882T+0.000029780T^2+5.068logT	4
log [H2] = -1.640 -124524/T^2 -777.19/T -0.0005501T +0.000007756T^2 -0.565logT	5
log [H2] = -1.544 -151109/T^2-752.389/T -0.0005868T +0.000007080T^2 0.532logT	6
log [H2] = 1.444 -273812/T^2 -3962.1/T +0.002401T +0.000001304T^2 +0.979logT	7
log [H2] = -1.654 -95456.8/T^2 -621.84/T -0.001257T +0.000007569T^2 –0.600logT	8
log [CO2] = -0.890 +7251.5/T^2 -1710.6/T+0.004188T +0.000002683T2 0.064logT	9
log [CO2] = -1.449 -40536/T^2 -2135.9/T +0.0065639T +0.000002725T2 -0.193logT	10
log [F-T] = -29.407 -1372240/T^2 +24737/T +0.10503T-0.000085048T^2 -11.296logT	11
logK_{H2S} = 24.229 +837819/T^2 -490.63/T -0.09836T -900.43/$T^{0.5}$ +0.00005500T^2+17.610logT	12
logK_{H2} = 10.650+768091/T^2-7651.7/T -0.04610T +94.908/$T^{0.5}$ +0.00003336T^2 +3.452logT	13
logK_{CO2} = 17.135 +726530/T^2 +65.396/T-0.06964T -731.50/$T^{0.5}$+0.00003912T^2+13.190logT	14
logK_{CH4} = 20.352 +853894/T^2 -444.61/T -0.08140T -856.26/$T^{0.5}$ +0.00004581T^2 +15.542logT	15

Activities of end-members in the epidote (epidote and clinozoisite), garnet (grossular and andradite) and prehnite (Al-prehnite and Fe-prehnite) solid solutions were used. The values were 0.8 and 0.2 for Epidote and clinozoisite respectively as well as for Al and Fe-prehnite. Grossular had 0.3 and 0.2 for andradite. Other minerals were taken to have unit activity.

4.2.2 Evaluation of gas concentrations versus the reservoir processes

a. Gas concentrations as a result of boiling and condensing processes

The calculations were done according to Reeds et al., (2012a and b). This was by inputting the reservoir temperatures as recorded from SOLVEQ run. CHILLER (CHIM) was run at the specified reservoir temperatures TEMP and a set limit SLIM so that no temperature increments takes place. The fluid pressures (PFLUID) in the pickup file was set lower than the saturation pressures while the temperature increments (STEP INCREM) for temperatures were set to -10 (decreasing temperatures). It must be noted that the oversaturated minerals as read out in SOLVEQ were suppressed to minimize their masking of the convergence of the equations. CHIM was then allowed to execute. The programme equilibrated with the gas phase and started boiling following STEP INCREM temperature drop and adjusted PFLUID. Considering that the enthalpy (ENTH) was set at zero, CHIM sets the current ENTH to be equal to the enthalpy of the aqueous phase at the given temperature. To ensure that the boiling remained isoenthalpic, the starting total enthalpy SENTH was set at zero, CHIM sets SENTH equal to the current total enthalpy ENTH. From the output (CHIMOUT.DAT, at full equilibration), the gas saturation was determined.

b. Fluid-fluid mixing ('Coolbrew' calculations)

The study first considered the mixing of aqueous solution into a high temperature reservoir with enthalpy constraint scenario (Reeds et al., 2012b). CHIM computed an enthalpy balance between the boiling solution and the mixer solution. The change of composition of the system (TOTAL MOLES was calculated as TOTAL MOLES + STEP INCREM * MIXER TOTAL MOLES) while the total current enthalpy of the system was also changed from ENTH to ENTH + STEP INCREM * MIXER TOTAL MOLES * ENTHW (enthalpy of the mixer solution). The mixing first resulted in the condensation of the gas phase at a constant temperature. Just like in the boiling evaluation, oversaturated minerals as read out in SOLVEQ were suppressed. According to Reeds et al., (2012b) once all the gas phase were condensed, CHIM proceeded in computing fluid-fluid mixing and temperature change by setting TEMPC to a non-zero value. This allowed CHIM to titrate a mixer solution of composition given by mixer total moles into the current solution of composition given by total moles. The composition of the mixer solution was in moles, except for water, mixer total moles, which were in kilograms.

c. Water- rock interaction (MINSOLV option)

The water-rock interaction option in CHIM option was enabled with MINSOLV being set to a non-zero value and allowing SiO_2, Fe_2O_3, FeO, MgO, CaO, Na_2O, FeS and NaCl as the reactants. The CHIM then read the names and amounts of reactants in the CHIMRUN file and their stoichiometries CHIM from the MINOX data file (Reeds et al., 2012b). At the start of a reaction calculation, the total mixer was set to zero while the composition of the system changed from TOTAL MOLES to TOTAL MOLES + STEP INCREM * WTPC * 0.01 * spec/mwox, where spec is the molar amount of a given component species in the reactant NOMOX, and mwox is the molecular weight of reactant NOMOX. For increments in moles, total moles are changed to TOTAL MOLES + STEP INCREM*WTPC*0.01*spec.

4.2.3 Evaluation of depth of gas breakout or bubble point

Gas breakout or two-phase conditions occurs at the depth at which the gas pressure plus water pressure exceeds the total pressure i.e. bubble point depth (Haizlip et al., 2012). In this case the gas pressure is given in the output files of CHIM programme whereas the water pressures were estimated using steam tables as follows:

$P_{liq} = P_{water}$@sat T ……..…….i

$P_{tot} = P_{gas} + P_{liq}$ ……...ii

The temperatures values were taken from the SOLVEQ output files and were assigned to the major feed zones as determined from the downhole temperature and pressure profiles of each well as shown in table 1 below.

5.0 RESULTS

The results are categorized into two parts. Part one presents the evaluation of the equilibrium states of the fluids in the wells considered whereas part 2 details the processes leading to gas evolution. These results are in form of gas pressure (bars) vs temperature graphs.

5.1 The equilibrium state of the fluids

The $LogH_2$ vs temperature curve has curves (Figure 6) defined by equation 5, 6, 7 and 8. The plotted results show that the study wells closely correlate mineral assemblages in equation 5 and 8 (see Table 1). OW-914 appears to be in near equilibrium as it plots close to the equation curve followed by OW-44. OW-915 and OW-724A appear to be out of equilibrium as they plot far from the equation

curves. These results agree with those by Arnorsson et al., (2010) where most of the wells in the field had their fluid concentrations of H_2 closely corresponding to equilibrium with mineral assemblages in 5 and 8. The gas concentration is low, ranging between -2.0 moles/kg in OW-915 and -2.5 moles/kg in OW-914 which closely corresponds to a range between -3 moles/kg to -5.5 moles/kg by (Arnorsson et al., 2010).

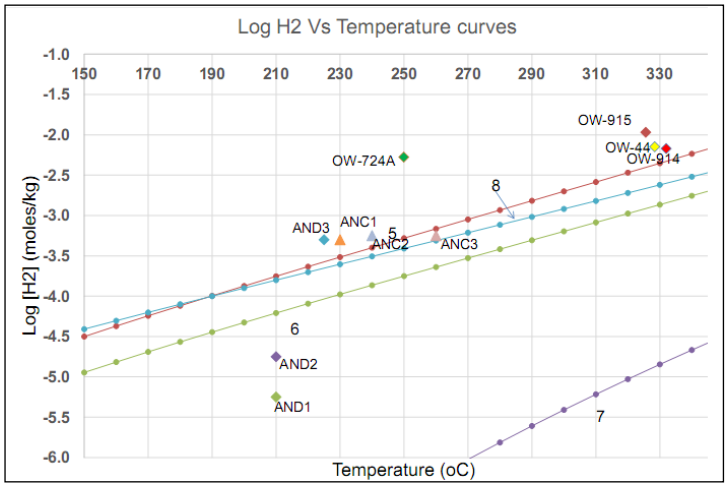

Figure 6: Calculated concentrations of H_2 in the total aquifer fluid of wells OW-44, OW-724A, OW-914 and OW-915.

The Log H_2S vs temperature graph has mineral curves (Figure 7) for 1, 2, 3 and 4. The wells plot in the temperature range between 300°C and 330°C. This is with the exception of OW-724A which plots at 250°C. OW-724A seems to be in equilibrium with mineral assemblage 1 and 4, OW-44 with mineral assemblage 2 and 3, OW-915 with mineral assemblage 3 whereas OW-914 seems to be in non-equilibrium with the mineral assemblage. The results still hold for Arnorsson et al., (2010) with the exception of OW-914 which seemed depleted with H_2S an indication of steam loss and therefore gas loss.

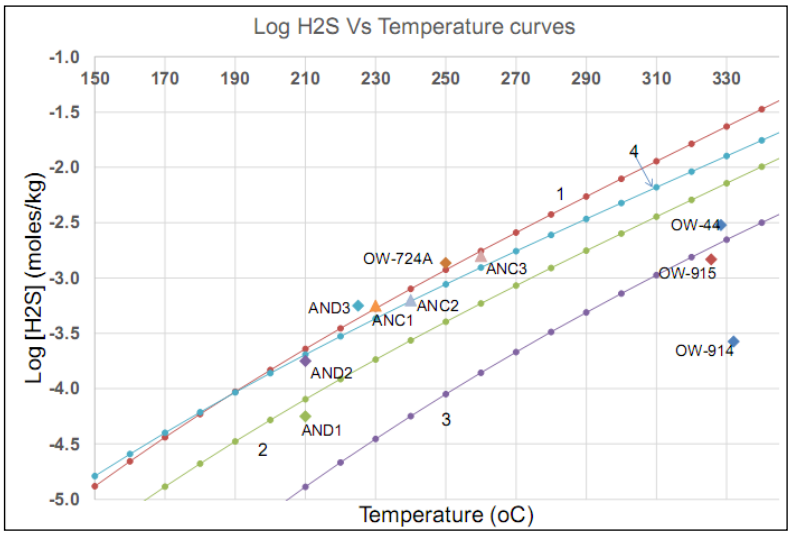

Figure 7: Calculated concentrations of H_2S in the total aquifer fluid of wells OW-44, OW-724A, OW-914 and OW- 915. AND and ANC are Arnorsson et al., (2010) data from Olkaria Domes and Olkaria Central field respectively. The numbers on the curves refer to the reactions in Table 1.

The Log CO_2 graph (Figure 8) is defined by two mineral assemblages 9 and 10. Two wells i.e. OW-914 and OW-915 are in equilibrium with mineral assemblages in equation 10. OW-44 plots way below mineral assemblage in equation 9 whereas OW-724A plots above the mineral assemblage in equation 10. This is an indication that OW-724A and OW-44 are in non-equilibrium. The values of concentration also give OW-44 to be having the smallest amount of gas whereas OW-914 has the highest amount. The findings concur with Arnorsson et al., (2010) where the Domes Sector had the highest CO2 concentration whose likely cause was the high flux of this gas from the magma heat source.

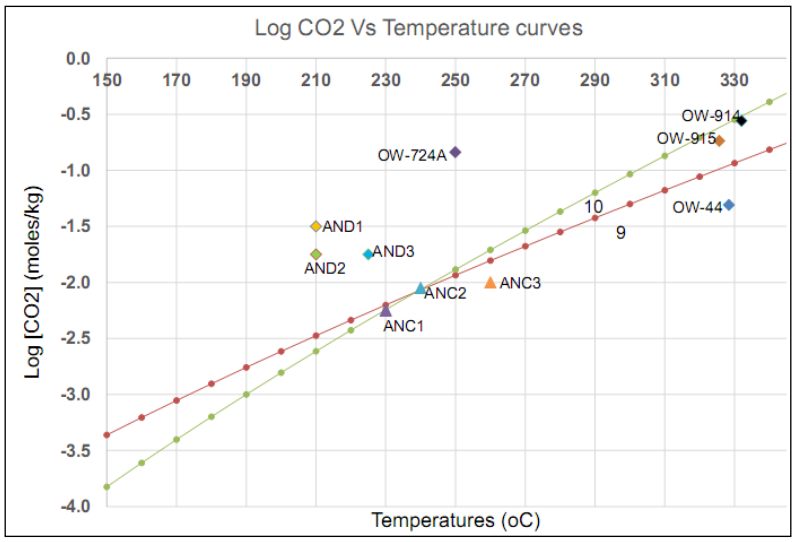

Figure 8: Calculated concentrations of CO_2 in the total aquifer fluid of wells OW-44, OW-724A, OW-914 and OW-915. AND and ANC are Arnorsson et al., (2010) data from Olkaria Domes and Olkaria Central field respectively. The numbers on the curves refer to the reactions in Table 1.

5.2 Gas concentrations and the reservoir processes in the wells

The reservoir processes considered were boiling, fluid-fluid mixing and titration. The plots for OW-44 indicate that boiling is the major process leading to evolution of gases. The gas pressures seem to increase steadily with temperatures, steadily rising from 2.4 and 50 bars. The mixing process comes in second. Unlike the boiling process, the curve remained leveled up to about 200°C before starting to increase. The curve on titration has almost similar trend but lesser values ranging between 0 and 2.4 bars (Figure 9).

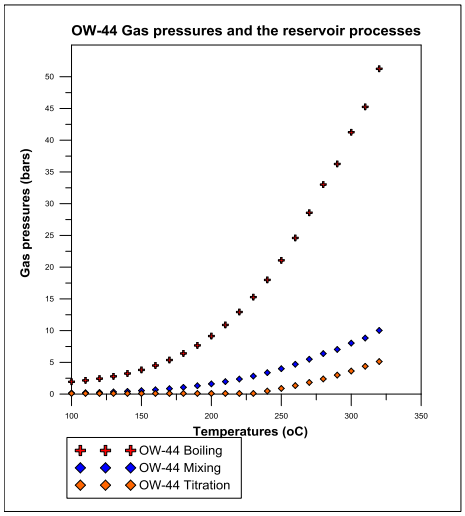

Figure 9: Gas pressures against the reservoir processes in OW-44.

OW-724A, just like OW-44 has boiling as the major process leading to gas evolution (Figure 10). The graph begins with a drug between 100°C and 120°C at a gas pressure value of about 0.1 bars before steadily rising to 37 bars. The mixing curve also experiences the same initial drag and later an increase but has lesser values between 0.1 and 17 bars compared to the boiling processes. The titration process start with a linear increase in the gas pressures up to around 180°C. The curve however shows a decline in the gas pressures between 180°C and 220°C. This is perhaps an indication of reducing reactants which later change to a steady increase reaching a high of 0.0016 bars.

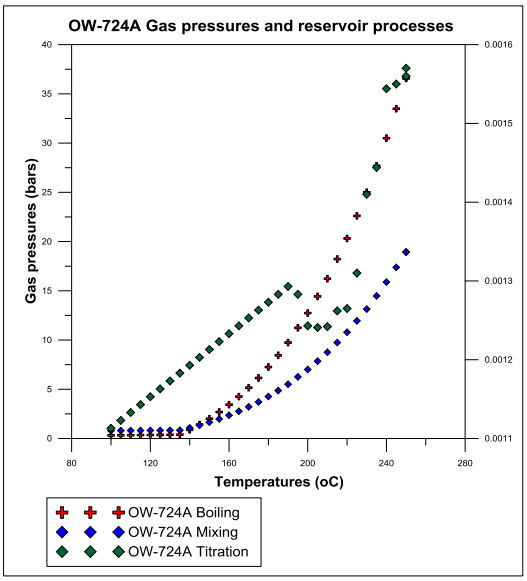

Figure 10: Gas pressures against the reservoir processes in OW-724A. The titration curve has been plotted on the secondary axis.

OW-914 has its resulting gas pressures due to boiling ranging between 10 and 92 bars (Figure 11). The mixing graph comes in second with values ranging between 0 and 50 bars. The titration curves give almost a zero gradient trend between 100°C and 200°C. This is followed by a slight increase to about 2.5 bars towards the end.

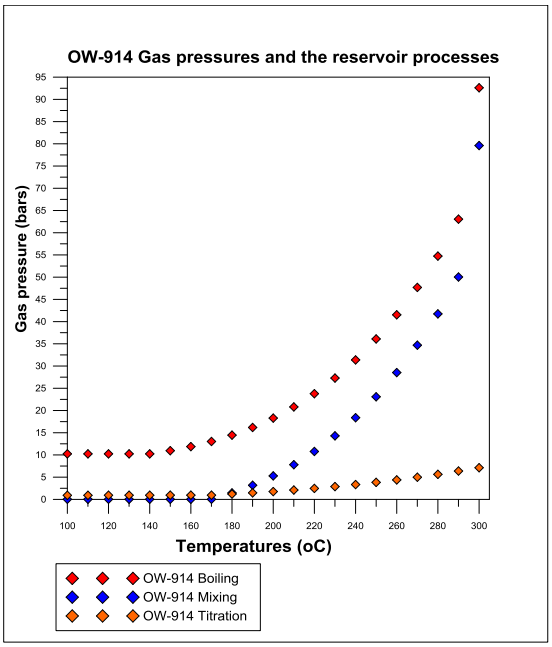

Figure 11: Gas pressures against the reservoir processes in OW-914.

OW-915 just like OW-914 has its gas pressures due to boiling steadily increasing reaching a high of 85 bars (Figure 12). The mixing curve show a slight increase in the gas pressure with temperature, recording of values between 0 and 10 bars. The titration curve has almost similar trends to OW-724A. The curve start with evidence of an increase in gas pressures to a temperature of 170°C, levels out to 210°C before starting to increase to a high of about 5 bars.

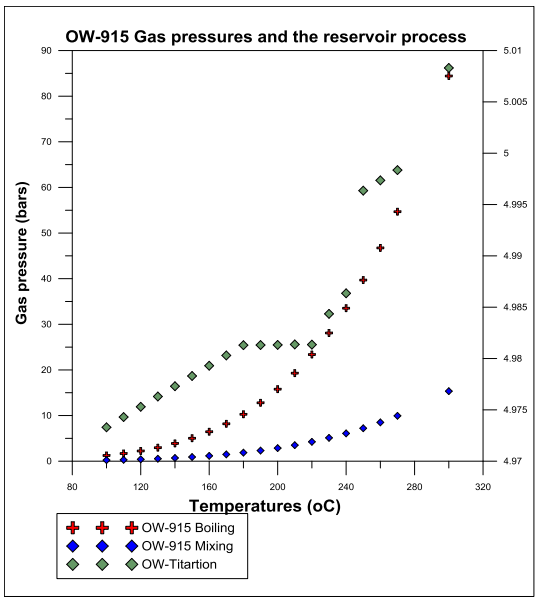

Figure 12: Gas pressures against the reservoir processes in OW-915. The titration curve has been plotted on the secondary axis.

The processes comparison curves (Figure 13) indicate boiling processes to be highest in magnitude in OW-914 followed by OW-915, OW-724A. OW-44 has the least amount of gas pressures generated. The mixing process gas evolution, on the other hand seems high in OW-914 followed by OW-724A then OW-915 and lastly OW-44. Titration processes just like the mixing ones are higher in OW-914. OW-915 comes in second followed by OW-44 then OW-724A.

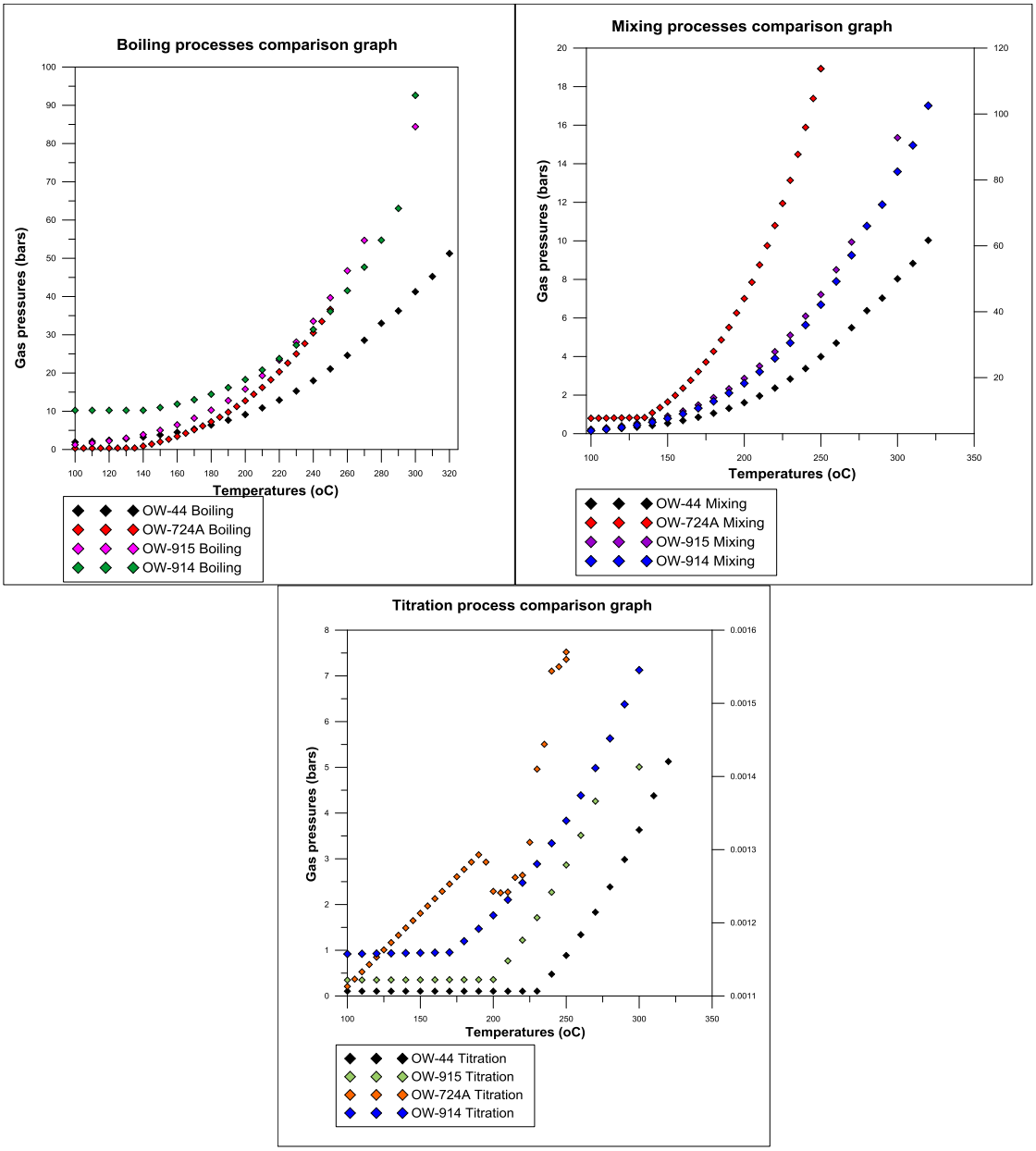

Figure 13: Reaction processes comparison graphs. The titration curve in OW-724A has been plotted on the secondary axis.

6.0 DEPTH OF GAS BREAKOUT OR BUBBLE POINT

The measured pressures at the major feed zones give the highest values of 175 bars in OW-44 followed by OW-915 at 150 bars, OW-914 at 100 bars and lastly OW-724A at 90 bars (Table 3). Using steam tables, pressure of the liquid (P_{liquid}) then added to the pressure of the gas P_{gas} from CHIM, the totals ranged between 52 bars in OW-44 to 92 bars in the OW-914. From the results, it is identifiable that OW-914 has its total pressure close to the downhole measured one indicating higher chances of gas break out at its major feed zone. OW-44 had the least chances as its total pressure was way less, at 52 bars compared to 175 bars (measured).

TABLE 3: Showing a comparison between measured and calculated pressures in the main feed zones

Well Name	Depth of major feed zone (m)	Pressure (bars)	P_{liquid} (bars)	$P_{gas\ (bars)}$	$P_{total\ (bars)}$
OW-44	2250	175	0.105	52	52
OW-724A	1700	90	0.002	36	36
OW-914	1500	100	0.025	92	92
OW-915	2300	150	0.035	84	84

6.0 DISCUSSION OF THE RESULTS

6.1 The equilibrium state of the fluids

The current study and that of Arnorsson et al., (2010) agree that the H_2 and H_2S gas concentrations are low in the Olkaria geothermal field. This is confirmed by minor values ranging between -2 to -3.5% by weight (Figure 6 and 7) indicating that the aquifer vapor fraction is insignificant. Arnorsson et al., (2010) attributes these low concentrations to steam loss resulting from the boiling of fluid flowing into these wells. OW-724A plotting way above the mineral assemblage curves in the H_2 whereas OW-914 plots way below in the H_2S graph. This is an indication that boiling, condensation and mixing, has resulted in non-equilibrium distributions of gas species (Arnorsson et al., 2010).

The CO_2 plot indicates that the calculated aquifer fluid CO_2 concentrations are in equilibrium as in the case of OW-914 and OW-915. OW-44, apart from being in non-equilibrium with the mineral assemblages has the least concentration (Figure 7). According to Arnorsson et al., (2010), the low CO_2 values as in OW-44 are due to insufficient supply of the gas to the fluid to saturate it with calcite. This case therefore reveals that the aquifer fluid CO_2 concentration is externally controlled that is, the flux into the geothermal fluid is either from a degassing magma or from the rock with which the geothermal fluid interacts or fumaroles or both. This is opposite with the case of OW-724A which plots above the equilibrium curves. This is an indication that the non-equilibrium in OW-724A maybe arising from a process of volcanic degassing below these areas with minor gas loss compared to OW-44.

6.2 Gas concentrations and the reservoir processes in the wells

The results points to boiling as the major process leading to evolution of gases (Figure 9, 10, 11 and 12). The increase in gases is as a result of elevated enthalpy resulting from the flow or gravity segregation of water and steam where the steam flow preferentially to the well leaving behind water or enhanced vaporization boiling where there is flow of heat from the rock to the fluid (Simsek et al., 2009). The former describes a scenario where there is boiling in the area around the well while the later is whenever the water has cooled by adiabatic boiling as a result of the pressure drop leading to generation of steam and gas (Simsek et al., 2009).

Titration process is dependent on both the boiling and mixing processes. According to Simsek et al., (2009) boiling in the upper portion of geothermal systems is usually accompanied by the transfer of acidic gases (CO_2 and H_2S) to the resultant steam. These gases then penetrate into the aquifer rocks or become condensed into shallow ground waters giving rise, with oxidation, to distinctive low pH sulfides and bicarbonate water which in turn reacts leading to evolution of gases. Mixing process, on the other hand, is characterized by incursion of cooler fluids. The fluids, once in the high temperature geothermal reservoir, come in contact with the reservoir rocks. This sets in chain of reactions where the fluids react with mineral components of the rocks leading to release of gases as shown in Figure 14 below.

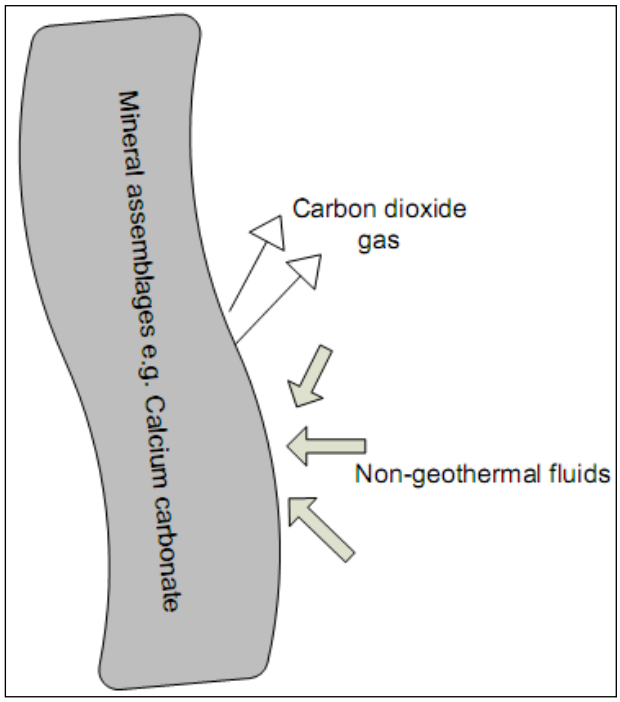

Figure 14: Schematic representations of reactions under the mixing processes. The grey area to represent the rock materials, thick arrows for the direction of incoming fluids and thinner ones for the direction for gases evolved.

From the graph, it is notable that the intensity of the processes increases with temperatures in the considered wells. This is so as temperatures act as catalysts for reactions leading to evolution of the gases (Haizlip et al., 2010). Here the reservoir temperatures act to increase the average kinetic energy of its constituent particles leading to the particles moving faster and colliding more frequently per unit time and possess greater energy when they collide. According to Haizlip et al., (2010) both of these factors increase the reaction rate hence increased gas evolution.

The comparison in the magnitude of this processes in the wells indicate that the impacts of the processes are highest in OW-914 and lowest in OW-44 (Fig. 13). This trend in OW-914 is attributed to the high temperature values of about 325°C such that chain reactions similar to those discussed in the mixing processes take place. This is further supported by the fact that this well has high injectivity of about 315lpm/bar, an indication of high permeability of the well. This acts to bring in fluids that in turn react with the mineral assemblages in the aquifer rocks leading to evolution of gases.

OW-44 had the least gas concentrations arising from the considered reservoir processes despite the fact that it has high downhole temperatures of about 300°C and considerably high injectivity. Hazil et al., (2010) attributes this to loss of gas from the deep fluid due to degassing and near surface boiling. Besides that, NH_3, H_2 and H_2S can be removed from the steam formed through boiling by processes like wall-rock interactions and solution into steam condensate. Then depending on how far the well is from the recharge zone, gases in the reservoir fluid tend to enter the vapor phase whenever possible (Simsek et al., 2009). Therefore, when boiling sets in, the initial steam formed contains majority of the dissolved gases thus the residual liquid is therefore highly depleted in dissolved gases and later stages of steam separation will contain increasingly lower concentrations of gases. Steam formed in the early stages of boiling is therefore characterized by higher gas content.

6.3 Depth of gas breakout or bubble point

This was meant to determine the potential impacts of the gases on the performance of the wells. The results (Table 3) indicate that likelihood of a gas breakout is highest in OW-914 and least in OW-44. This therefore is an indication that OW-914 is likely to experience calcite scaling at its major feed zone at 1500m depth, considering the type of waters feeding the well. This finding agrees with a dynamic survey carried out in OW-914 well in 2014 (Figure 15). The results pointed to a calcite scaling potential in the depths between 1200 and 1800m. According to Akin et al., (2015) due to pressure drop, thermal fluids tend start to boiling and degassing of CO_2 as the fluids rise in a wellbore. When the initial gas bubbles are formed, CO_2 exsolution affects the pH together with the carbonate species leading to the thermal fluid becoming saturated to calcite.

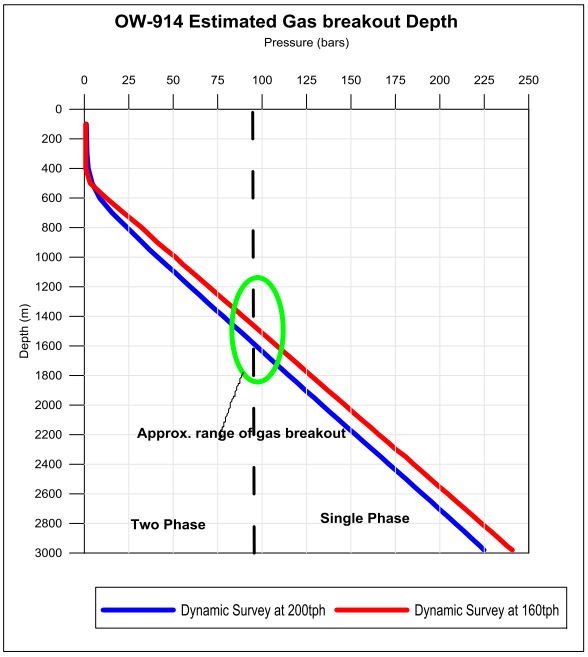

Figure 15: Estimated gas breakout depth in OW-914 from the dynamic surveys.

7.0 POSSIBLE RESERVOIR MANAGEMENT OPTIONS

Continuous exploitation has tended to increase the concentration of non-condensable gases in the reservoir (Moya and Yock, 2005). Moya and Yock (2005) adds that this in turn need the establishment of a program of detailed monitoring of the non-condensable gases at each well in order to determine the principal causes of the increase, and to select the best injection and production strategies to improve on the existing operating conditions. This study has indicated that the principal cause of the increase in non-condensable gases is pressure decline in the reservoir leading to depressurization boiling. In order to minimize this tendency, two different strategies for the different parts of the Olkaria geothermal field were considered (Figure 16). First, there is need to put in place well programmed and targeted reinjection. This will see an increasing the volume of fluids injected in the eastern sector (represented by well OW-44). The immediate response here would be the decrease in the enthalpy of the wells and gases evolution.

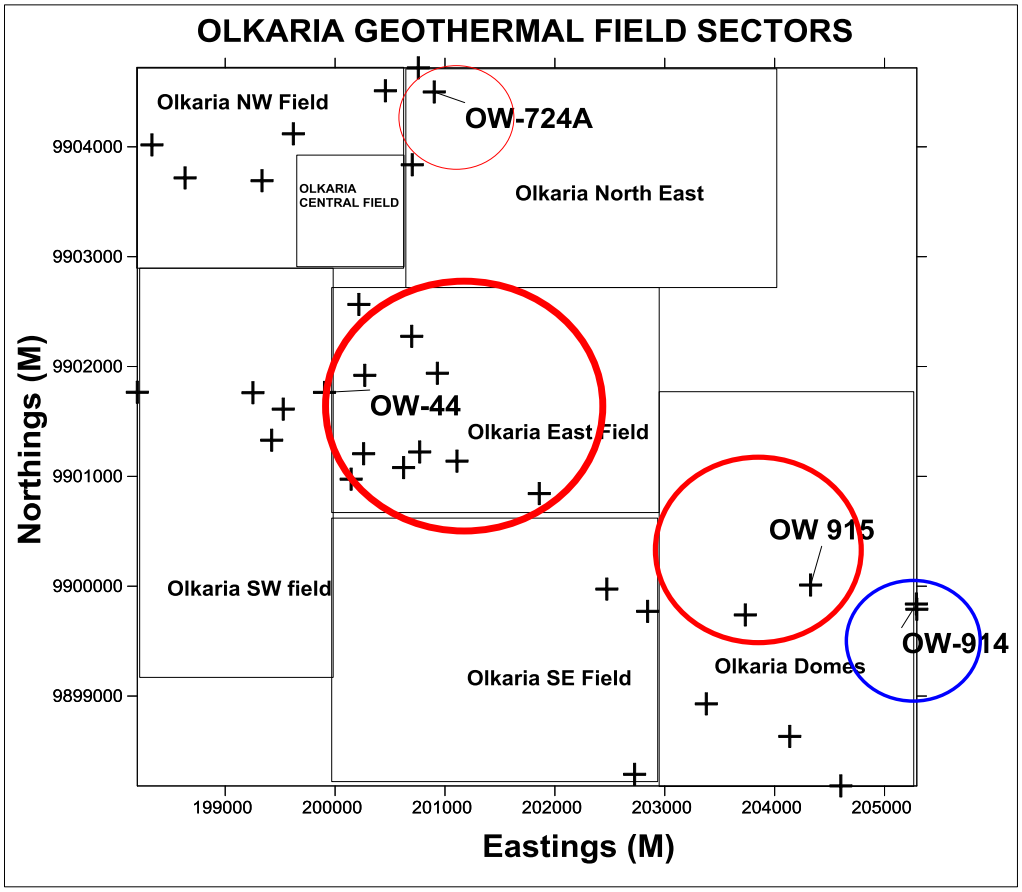

Figure 16: Management options for different parts of the field. Red eclipses for reinjection while the blue one is for reduced flow from wells and inhibition.

For wells around and with similar chemistry like OW-914, two options are applicable. First the management by operating the wells at a minimum flow rate (or even to close them). According to Moya and Sanchez (2005) this will enable reduction in the pressure drop and consequently the non-condensable gas evolution due to depressurization boiling. This will also lead to a lowered scaling point and or reduced numbers of work over as demonstrated in Figure 17.

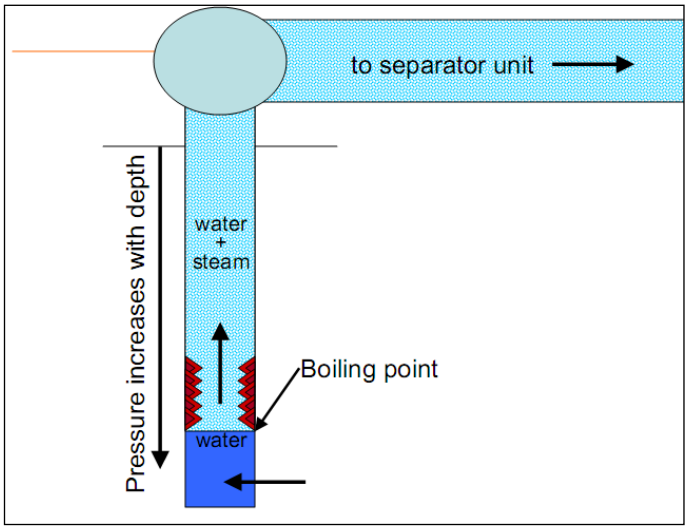

Figure 17: Showing lowered boiling point with decreased well head pressures (UNU-GTP 2015 lecture notes).

The second option will be to consider chemical inhibitors dosing. According to Haizlip et al., (2012) successful scale mitigation in the wellbore requires that the inhibitor is injected into the flowing well through capillary tubing at depths 10-50m below the estimated gas breakout depth preferably within the casing (Figure 18). The inhibitors act by poisoning the growth of scale.

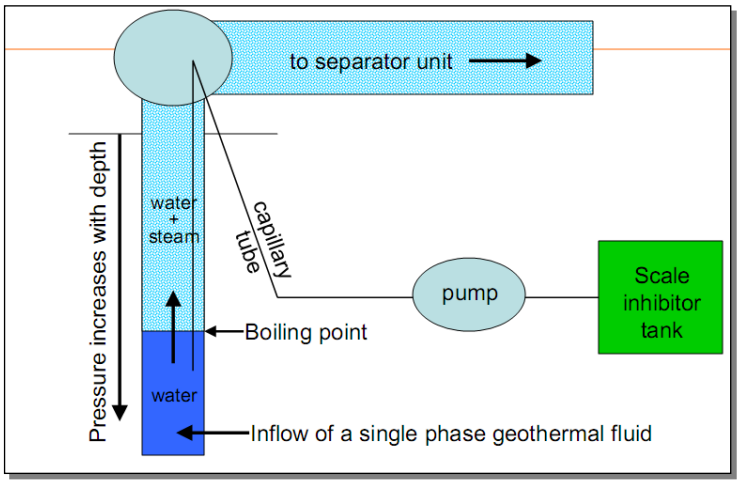

Figure 18: Showing an inhibitor injection set up (UNU-GTP 2015 lecture notes).

8.0 CONCLUSIONS

The study concludes that

- The gas species are not in equilibrium with the mineral assemblages due to processes of boiling, condensation and mixing
- Gas concentration values are low for the east field as represented by OW-44
- The CHIM evaluation show boiling as the major process leading to evolution of gases
- OW-44 had the least gas concentrations arising from the considered reservoir processes due to degassing and near surface boiling. Besides the removal of NH_3, H_2 and H_2S through reaction with steam condensate
- Gas breakout is most likely in OW-914 and least in OW-44.
- Different strategies for the different parts of the Olkaria geothermal field. That is increased volume of fluids injected in the eastern sector (represented by well OW-44).
- Area around OW-914 to be managed by operating the wells at a minimum flow rate (or even to close them) or use of chemical inhibitors

REFERENCES

Akin T., Guney A., and Kargi H. : Modeling of Calcite Scaling and Estimation of Gas Breakout Depth in a Geothermal Well by Using PHREEQC. PROCEEDINGS, Fortieth Workshop on Geothermal Reservoir Engineering Stanford University, Stanford, California, January 26-28, (2015) SGP-TR-204.

Angcoy, Jr., E.C. : Geochemical Modeling of the High-Temperature Mahanagdong Geothermal Field, Leyte, Philippines, Master's thesis, Faculty of Science, University of Iceland, (2010) pp. 126.

Arnórsson, S., Angcoy, Jr., E.C., Bjarnason, J.Ö., Giroud, N., Gunnarsson, I., Kaasalainen, H., Karingithi, C., and Stefánsson, A.: Gas chemistry of volcanic geothermal systems. *Proceedings World Geothermal Congress* (2010), Bali, Indonesia.

Bienkowski, R.: Genese hochsaurer Fluide im Geothermalfeld von Los Humeros, Zentral-Mexiko. Diplomarbeit (M.Sc. Thesis), Institut für Angewandte Geowissenschaften, Technische Universität Darmstadt (2003).

Clarke, M. C. G., Woodhall, D. G., Allen, D. and Darling, G.,: Geological, volcanological and hydogeological controls of the occurrence of geothermal activity in the area surrounding Lake Naivasha, Kenya. Ministry of Energy report (1990).

Clarke, M. C. G., Woodhall, D. G., Allen, D. and Darling, G.,: Geological, volcanological and hydogeological controls of the occurrence of geothermal activity in the area surrounding Lake Naivasha, Kenya. Ministry of Energy report (1990).

Fernandez-Prini, R., Alvarez, J.L. and Harvey, A.H.: Henry´s constants and vapor-liquid distribution constants for gaseous solutes in H_2O and D_2O at high temperatures. J. Phys. Chem. Ref. Data, 32 (2003), 903-916.

Haizlip, J.R., Guney, A., Tut Haklidir, F.S., Garg, S.K.,: The impact of high non condensable gas concentrations on well performance Kizildere geothermal reservoir, Turkey, Proceedings, 37th Workshop on Geothermal Reservoir Engineering, Stanford University, Stanford, CA (2012).

Karingithi, C.W., 2000: Geochemical characteristics of the Greater Olkaria geothermal field, Kenya. Report 9 in: Geothermal Training in Iceland 2000. UNU G.T.P., Iceland, 165-188.

Karingithi, C.W.: Hydrothermal mineral buffers controlling reactive gases concentration in the Greater Olkaria geothermal system, Kenya. United Nations University, Report 2, Geothermal Programme MSc thesis, University of Iceland, (2002) 46-47.

KenGen,: Conceptualized model of the Olkaria geothermal field (compiled by Muchemi, G.G.) The Kenya Electricity Generating Company, Ltd, internal report, (1999) 46 pp.

Lagat J., Arnorsson S. and Franzson H.: Geology, Hydrothermal Alteration and Fluid Inclusion Studies of Olkaria Domes Geothermal Field, Kenya. Proceedings World Geothermal Congress (2005). Antalya, Turkey, 24-29 April 2005.

Moya, P. and Sánchez, E.: "Non-condensable Gases at the Miravalles Geothermal Field", PROCEEDINGS, Thirtieth Workshop on Geothermal Reservoir Engineering Stanford University, Stanford, California, January 31-February 2, (2005).

Moya, P. and Yock, A.: "First Eleven Years of Exploitation at the Miravalles Geothermal Field", PROCEEDINGS, Thirtieth Workshop on Geothermal Reservoir Engineering Stanford University, Stanford, California (2005), January 31-February 2, 2005.

Mungania, J.: Preliminary field report on geology of Olkaria volcanic complex with emphasis on Domes area field investigations. Kenya Power Company internal report (992).

Naylor, W. I.: The geology of the Eburru and Olkaria geothermal projects. Geothermal Resource Exploration Prospects, UNDP report. Restricted (1972).

Ogoso-Odongo, M., E.: Geology of Olkaria geothermal field. Geothermics, (1986) Vol. 15, 741-748.

Omenda, P. A.: The geological structure of the Olkaria west geothermal field, Kenya. Stanford Geothermal Reservoir Engineering Workshop, (1994) Vol 19, 125-130.

Omenda, P. A.: Anatectic origin for Comendite in Olkaria geothermal field, Kenya Rift; Geochemical evidence for syenitic protholith. African Journal of Science and Technology. Science and Engineering series, (2000) Vol. 1, 39-47.

Ouma, P. A.: Reservoir Engineering Report for Olkaria Domes Field. Kenya Electricity Generating Company Ltd., internal report, (1999) 54 pp.

Robie, R.A. and Hemingway, B.S.: Thermodynamic properties of minerals and related substances at 298.15 K and 1 bar (105 Pascals) pressures and at higher temperatures. U.S. Geol. Surv. Bull., 2131 (1995).

Shackleton, R. M.: Precambrian collision tectonics in Africa. In: Coward, M. P. and Ries, A. C. (eds.). CollisionTectonics. Geol. Soc. Spec. Publ. No. 19, (1986) 329-349.

Simsek, S., Parlaktuna, M. and Akın, S., 2009: Data gathering and evaluation of Kizildere geothermal field, prepared report for Zorlu Energy, 13p.

Smith, M. and Mosley, P.: Crustal heterogeneity and basement influence on the development of the Kenya rift, East Africa. Tectonics, (1993) Vol. 12, 591-606.

Thompson, A.O. and Dodson, R.G.: Geology of the Naivasha area. Geological Survey Kenya, (1963) report No.55.

VIRKIR Consulting Group: Geothermal development at Olkaria (1980). Report prepared for Kenya Power Company.

West-JEC: The Olkaria Optimization Study (Phase II) – Final reservoir analysis report. West Japan Engineering Consultants, (2009) Inc., 301 pp.

Reed M. H., Spycher N. F. and Palandri J.: SOLVEQ-XPT: A Computer Program for Computing Aqueous-Mineral-Gas Equilibria. Department of Geological Sciences University of Oregon Eugene, (2012a) or 97403.

Reed M. H., Spycher N. F. and Palandri J.: Users Guide for CHIM-XPT: A Program for Computing Reaction Processes in Aqueous-Mineral-Gas Systems and MINTAB Guide (Ver 2.43). Department of Geological Sciences University of Oregon Eugene, (2012b) or 97403.